Cell Reports, Volume *16*

Supplemental Information

The *miR-17∼92* microRNA Cluster Is a Global Regulator of Tumor Metabolism

Said Izreig, Bozena Samborska, Radia M. Johnson, Alexey Sergushichev, Eric H. Ma, Carine Lussier, Ekaterina Loginicheva, Ariel O. Donayo, Maya C. Poffenberger, Selena M. Sagan, Emma E. Vincent, Maxim N. Artyomov, Thomas F. Duchaine, and Russell G. Jones

Izreig *et al.*, Supplementary Information

Figure S1, Related to Figure 1. Validation of cell lines with altered *miR-17~92* expression.

(A) Validation of recombination and deletion of the *miR-17~92* locus in Eμ-Myc lymphoma cells. *miR-17~92*$^{fl/fl}$ cells expressing the Cre-ERT2 transgene were cultured without (-) or with (+) 4-OHT, and excision of the *miR-17~92* gene was confirmed by PCR using genomic DNA from cell clones. The wild type (*fl/fl*) and deleted (*Δ/Δ*) alleles are indicated.

(B) Expression of *miR-17~92* miRNA components in Eμ-Myc lymphoma cells. Shown are relative expression of individual mature miRNAs of the *miR-17~92* cluster in *fl/fl* and *Δ/Δ* cells as determined by qPCR. Transcript levels were determined relative to U6 sRNA, and normalized to expression levels observed in *fl/fl* cells (arbitrarily set to 1). Data represent the mean ± SEM for triplicate biological samples.

(C) Heat map of mature miRNAs expression for miRNAs of the *miR-17~92*, *miR-106a~363*, and *miR106b~25* miRNA clusters in *fl/fl* and *Δ/Δ* cells as determined by RNA-sequencing. RNA-seq counts for each sample are shown in the inset.

(D) *In vitro* growth curve of *fl/fl* and *Δ/Δ* Eμ-Myc lymphoma cells. Data represent the mean ± SEM for triplicate biological samples.

(E) Viability of *fl/fl* and *Δ/Δ* Eμ-Myc lymphoma cells after 48h of culture from the experiment in (D). Data represent the mean ± SEM for triplicate biological samples.

(F) Immunoblot for metabolic enzyme expression on lysates from *fl/fl* and *Δ/Δ* Eμ-Myc lymphoma cells. Actin levels are shown as a control for protein loading. HK2, hexokinase-2; LDHA, lactate dehydrogenase A; GLS1, glutaminase-1; GLS2, glutaminase-2.

(G) Cell size of *fl/fl* and *Δ/Δ* Eμ-Myc lymphoma cells as determined by forward scatter (FSC) using flow cytometry.

(H) Expression of *miR-17~92* miRNA components in Raji cells expressing a control (Ctrl) or *miR-17~92* overexpression construct (*17~92*) as determined by qPCR. Expression was set relative to individual mature miRNA levels in Raji control cells. Data represent the mean ± SEM for triplicate biological samples.

(I) *In vitro* growth curve of Raji cells expressing control vector (Ctrl) or ectopic expression of *miR-17~92* (*17~92*). Data represent the mean ± SEM for triplicate biological samples.

(J) Viability of Raji cells after 48h of culture from the experiment in (I). Data represent the mean ± SEM for triplicate biological samples.

Figure S2, Related to Figure 2. Gene expression analysis of *miR-17~92*-deficient Eμ-Myc lymphoma cells.

(A) Scatter plot of log2 fold changes between *fl/fl* and *Δ/Δ* Eμ-Myc lymphoma cells (on the y-axis) versus the mean of normalized counts on the x axis. Each dot represents an individual gene, with differentially expressed genes having an adjusted p value of < 0.01 highlighted in red. The complete list of differentially expressed genes is summarized in **Table S1**.

(B) Heatmap of differentially expressed TCA cycle pathway genes in *fl/fl* versus *Δ/Δ* Eμ-Myc lymphoma cells (*p value < 0.01*).

(C) Heatmap of differentially expressed genes of the OXPHOS pathway in *fl/fl* versus *Δ/Δ* Eμ-Myc lymphoma cells (*p value < 0.01*).

(D) Heatmap of all differentially expressed MYC target genes between *fl/fl* and *Δ/Δ* Eμ-Myc lymphoma cells (*p value < 0.01*) from Figure 2B. The complete list of differentially expressed genes is summarized in **Table S2**.

Figure S3, Related to Figure 3. Expression of the glucose transporters Slc2a1 and Slc2a3 in Eμ-Myc lymphoma cells.

Expression of the glucose transporters Slc2a1 (Glut1, *left*) and Slc2a3 (Glut3) in *fl/fl* and *Δ/Δ* Eμ-Myc lymphoma cells, as measured by RNA-sequencing analysis from the dataset described in **Figure 2**.

Figure S4, Related to Figure 4. Central carbon metabolism is regulated by the *miR-17* family components of *miR-17~92*.

(A) Expression of mature *miR-17~92* miRNA components in addback Eμ-Myc lymphoma cell lines from Figure 4B. Shown are relative expression (as determined by qPCR) of individual mature miRNAs of the *miR-17~92* cluster in *fl/fl*, *Δ/Δ*, and *Δ/Δ* lymphoma cells expressing the *miR-17~92* constructs described in Figure 4A. Transcript levels were determined relative to U6

sRNA, and normalized to expression levels observed in *fl/fl* cells (arbitrarily set to 1). Data represent the mean ± SEM for triplicate biological samples.

(B-C) Relative glutamine consumption (B) and ammonia production (C) in the indicated cell lines grown as in Figure 4C. Cells were grown in complete medium for 48 hours, and glutamine and ammonia levels in extracellular medium were measured. Metabolite levels were normalized to cell number, and expressed relative to metabolite levels in control cells (*fl/fl*). Data represent the mean ± SEM for biological triplicates.

(D) Metabolite isotopomer distribution of lactate, citrate, and glutamate for *fl/fl*, *Δ/Δ* (Ctrl), and *Δ/Δ* addback lymphoma cells expressing the full *miR-17~92* cluster (*+17~92*) or the cluster lacking *miR-17/20* (*+Δ17,20*) cultured with medium containing U-[^{13}C]-glucose, as in Figure 4F.

(E) GC-MS analysis of pyruvate and fumarate in *fl/fl* and *Δ/Δ* addback lymphoma cells following culture with U-[^{13}C]-glucose as in Figure 4F. *Left*, total abundance of unlabelled (^{12}C, white bar) and ^{13}C-labelled (^{13}C, black bar) pyruvate and fumarate in *fl/fl* and *Δ/Δ* addback lymphoma cells. Metabolite abundance was made relative to control (*fl/fl*) cells, and represent the mean ± SEM for triplicate samples. *Right,* isotopomer distribution for pyruvate and fumarate in *fl/fl* and *Δ/Δ* addback lymphoma cells.

(F) Metabolite isotopomer distribution of lactate, citrate, and glutamate for *fl/fl*, *Δ/Δ* (Ctrl), and *Δ/Δ* addback lymphoma cells expressing the full *miR-17~92* cluster (*+17~92*) or the cluster lacking *miR-17/20* (*+Δ17,20*) cultured with medium containing U-[^{13}C]-glutamine, as in Figure 4G.

(G) GC-MS analysis of fumarate and malate in *fl/fl* and *Δ/Δ* addback lymphoma cells following culture with U-[^{13}C]-glutamine as in Figure 4G. *Left*, total abundance of unlabelled (^{12}C, white

bar) and ^{13}C-labelled (^{13}C, grey bar) fumarate and malate in *fl/fl* and *Δ/Δ* addback lymphoma cells. Metabolite abundance was made relative to control (*fl/fl*) cells, and represent the mean ± SEM for triplicate samples. *Right,* isotopomer distribution for U-[^{13}C]-glutamine-derived fumarate and malate in *fl/fl* and *Δ/Δ* addback lymphoma cells.

Statistics for all figures are as follows: *, $p<0.05$; **, $p<0.01$; ***, $p<0.001$.

Figure S5, Related to Figure 5. Validation of LKB1 as a *miR-17* target.

(A) Western blot of Pten, Akt (total and phospho-S473), and actin protein levels in *fl/fl* and *Δ/Δ* Eμ-Myc lymphoma cells.

(B) Schematic of the *miR-17* consensus target sequence and conservation in the *Stk11* 3'UTR across mammalian species.

(C) Schematic depicting the location of the *miR-17* binding element in the short (S1) and long (L1) isoforms of the mouse *Stk11* 3' UTR.

(D) Luciferase reporter assays of the *Stk11* 3'UTR. 293T cells expressing FLAG-Ago2 (293T-Ago2) were transfected with empty vector (EV) or luciferase reporter constructs for the short (S1) or long (L1) variants of the *Stk11* 3'UTR containing either wild type (WT) or mutated (MUT) *miR-17* family recognition site as in Figure 5A. Shown is the mean ± SEM for the FLuc/RLuc ratio for triplicate samples, normalized to control cells (EV).

(E) Schematic of the various *Stk11* 3' UTR constructs used in Figure 5C.

Statistics for all figures are as follows: *, $p<0.05$; **, $p<0.01$; ***, $p<0.001$.

Figure S6, Related to Figure 7. Knockdown of LKB1 expression restores metabolic activity in *Δ/Δ* lymphoma cells.

(A) Relative glucose consumption (left) and lactate production (right) of control (*fl/fl*) or *Δ/Δ* cells expressing control (Ctrl) or LKB1 shRNAs following 48 hours of culture. Data represent the mean ± SEM for biological triplicates, and were normalized to cell number. Metabolite levels for all samples were expressed relative to levels in *fl/fl* cells .

(B) Relative glutamine consumption (left) and ammonia production (right) for cells cultured as in **Figure S6A**.

(C) GC-MS analysis of U-[^{13}C]-glucose-derived metabolites in control (*fl/fl*) or *Δ/Δ* cells expressing control (Ctrl) or LKB1-specific shRNAs, related to **Figure 7C**. *Top*, metabolite isotopomer distribution of lactate, citrate, and glutamate following 2 hours of culture with medium containing U-[^{13}C]-glucose. *Middle*, relative abundance of unlabelled (white bar) and ^{13}C-glucose-derived (black bar) pyruvate and fumarate. *Bottom*, metabolite isotopomer distribution of pyruvate and fumarate.

(D) GC-MS analysis of U-[^{13}C]-glutamine-derived metabolites in control (*fl/fl*) or *Δ/Δ* cells expressing control (Ctrl) or LKB1-specific shRNAs, related to **Figure 7D**. *Top*, metabolite isotopomer distribution of glutamate, citrate, and aspartate following 2 hours of medium containing U-[^{13}C]-glutamine. *Middle*, relative abundance of unlabelled (white bar) and ^{13}C-glucose-derived (black bar) fumarate and malate. *Bottom*, metabolite isotopomer distribution of fumarate and malate.

Statistics for all figures are as follows: *, $p<0.05$; **, $p<0.01$; ***, $p<0.001$.

Figure S1, Related to Figure 1. Validation of cell lines with altered *miR-17~92* expression.

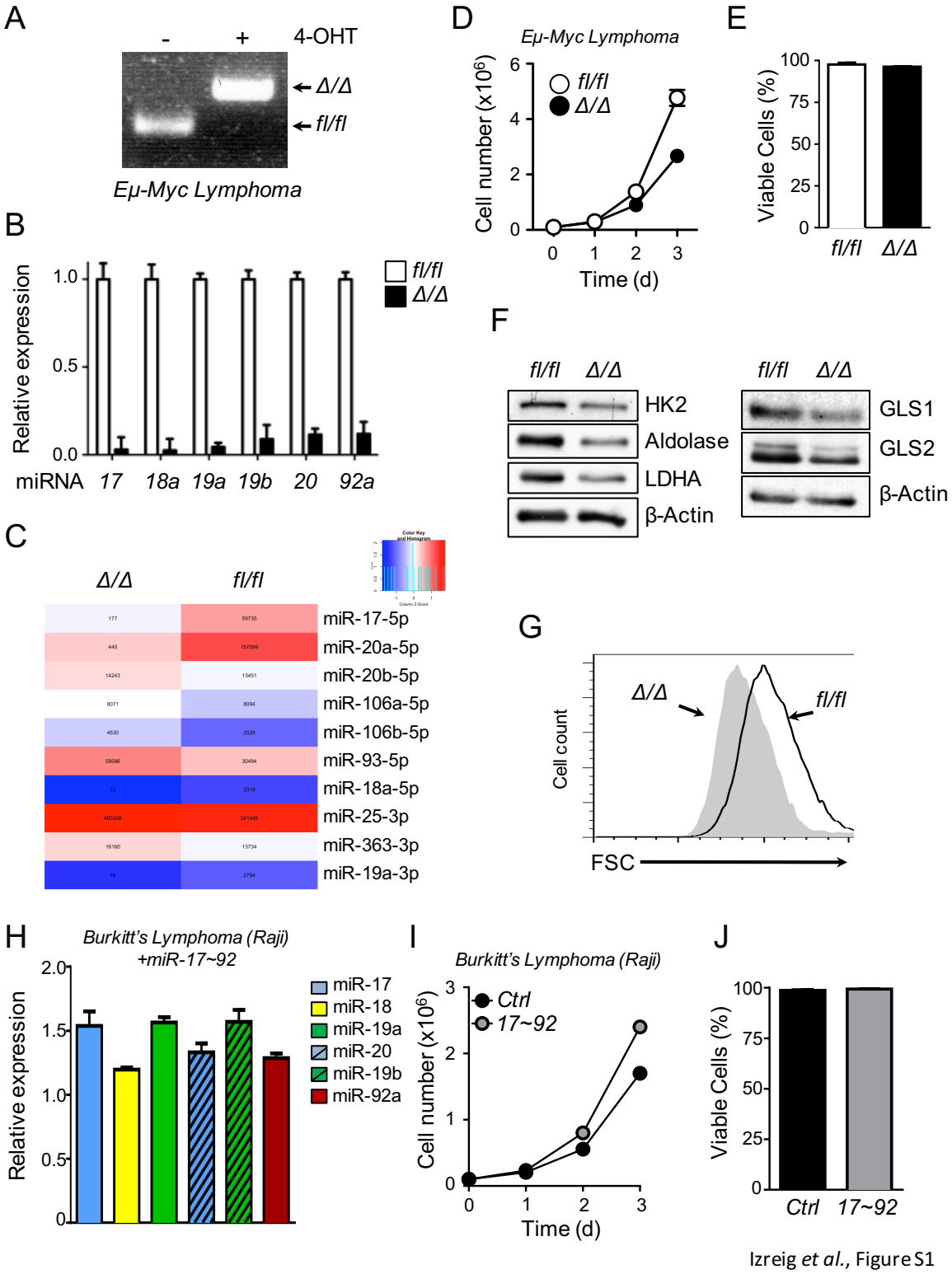

Izreig *et al.*, Figure S1

Figure S2, Related to Figure 2. Gene expression analysis of *miR-17~92*-deficient Eμ-Myc lymphoma cells.

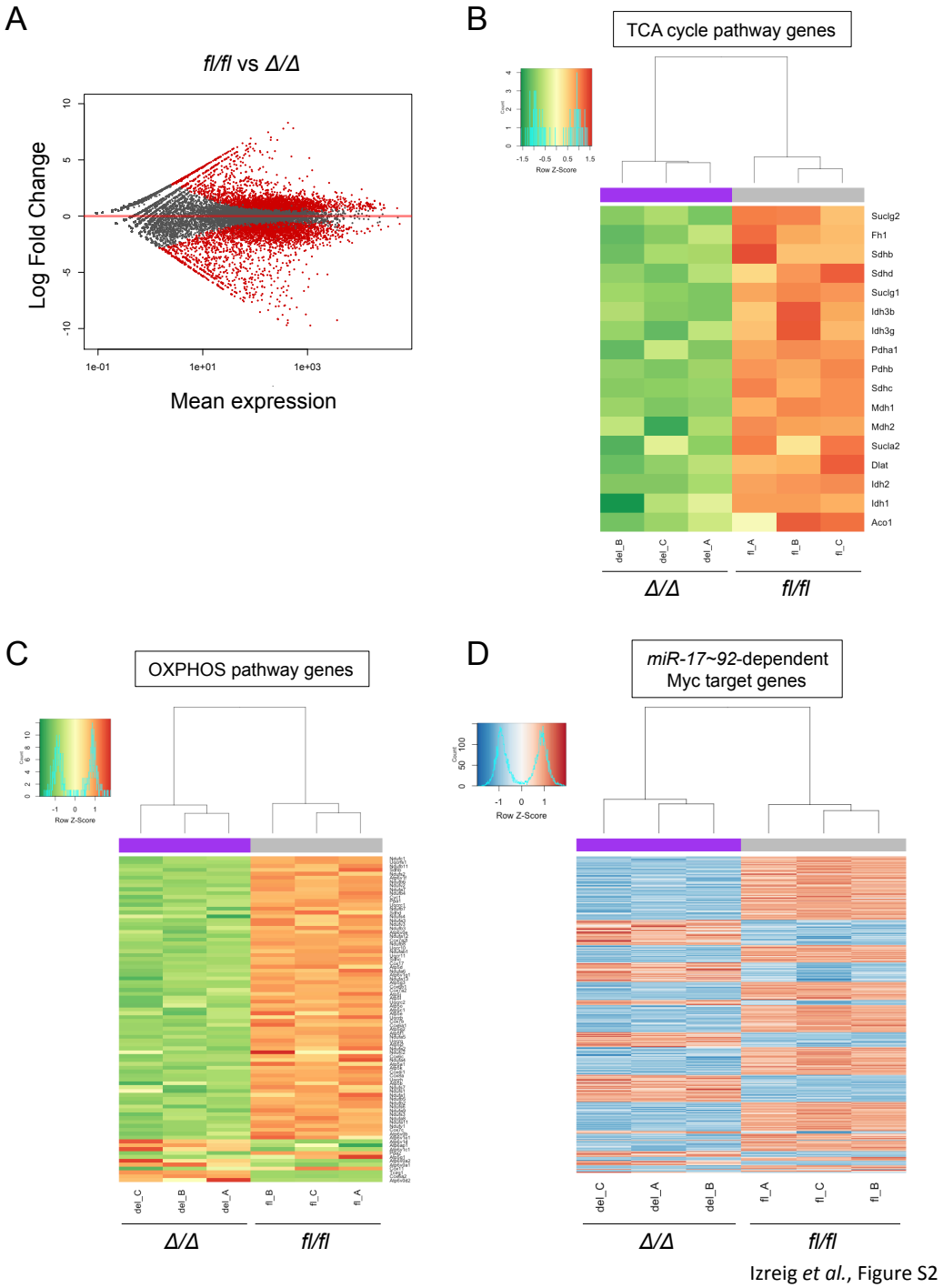

Izreig *et al.*, Figure S2

Figure S3, Related to Figure 3. Expression of the glucose transporters Slc2a1 and Slc2a3 in Eμ-Myc lymphoma cells.

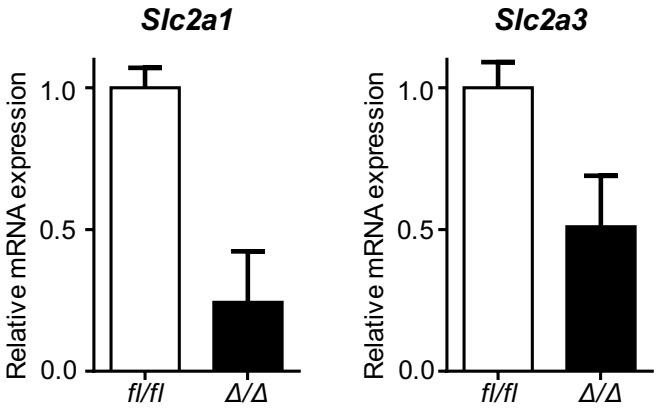

Izreig *et al.*, Figure S3

Figure S4, Related to Figure 4. Central carbon metabolism is regulated by the *miR-17* family components of *miR-17~92*.

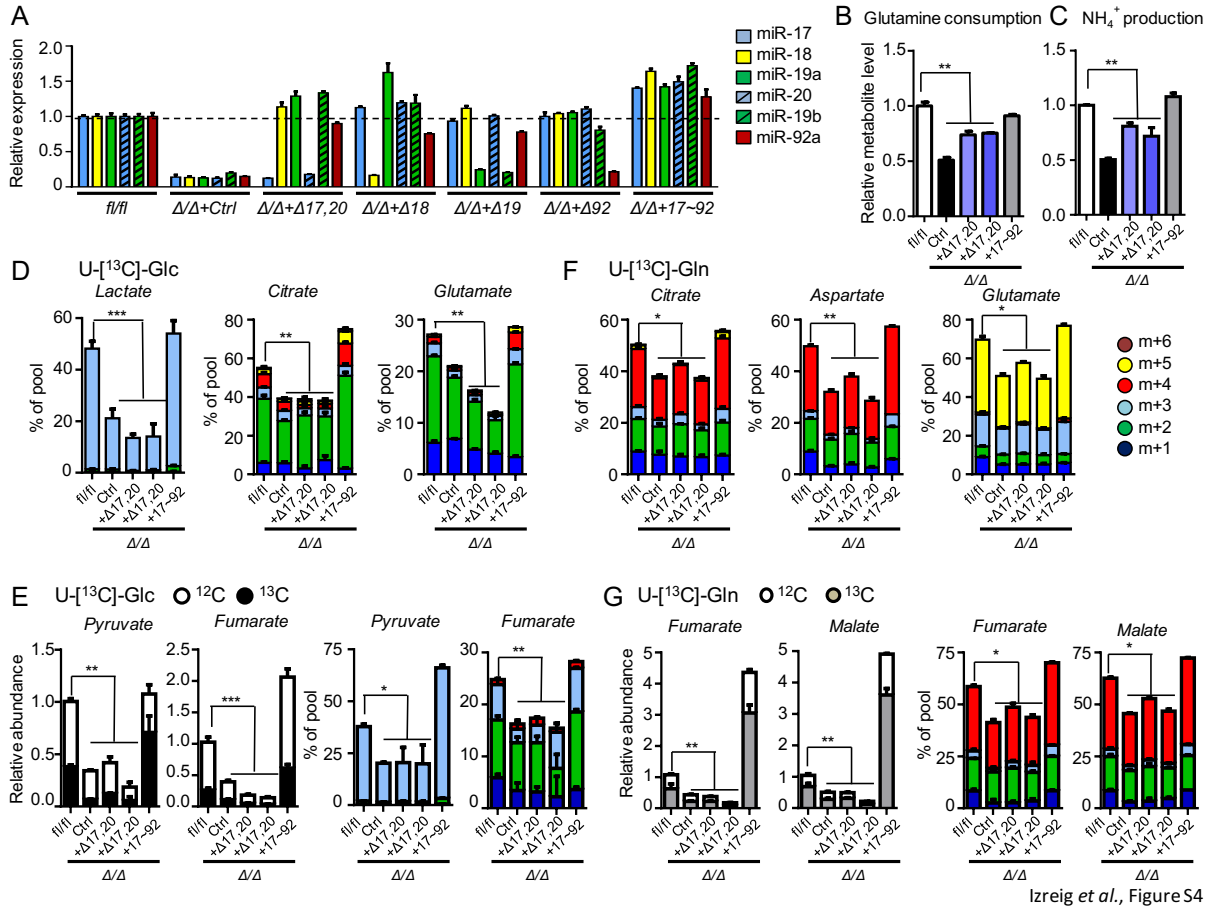

Figure S5, Related to Figure 5. Validation of LKB1 as a *miR-17* target.

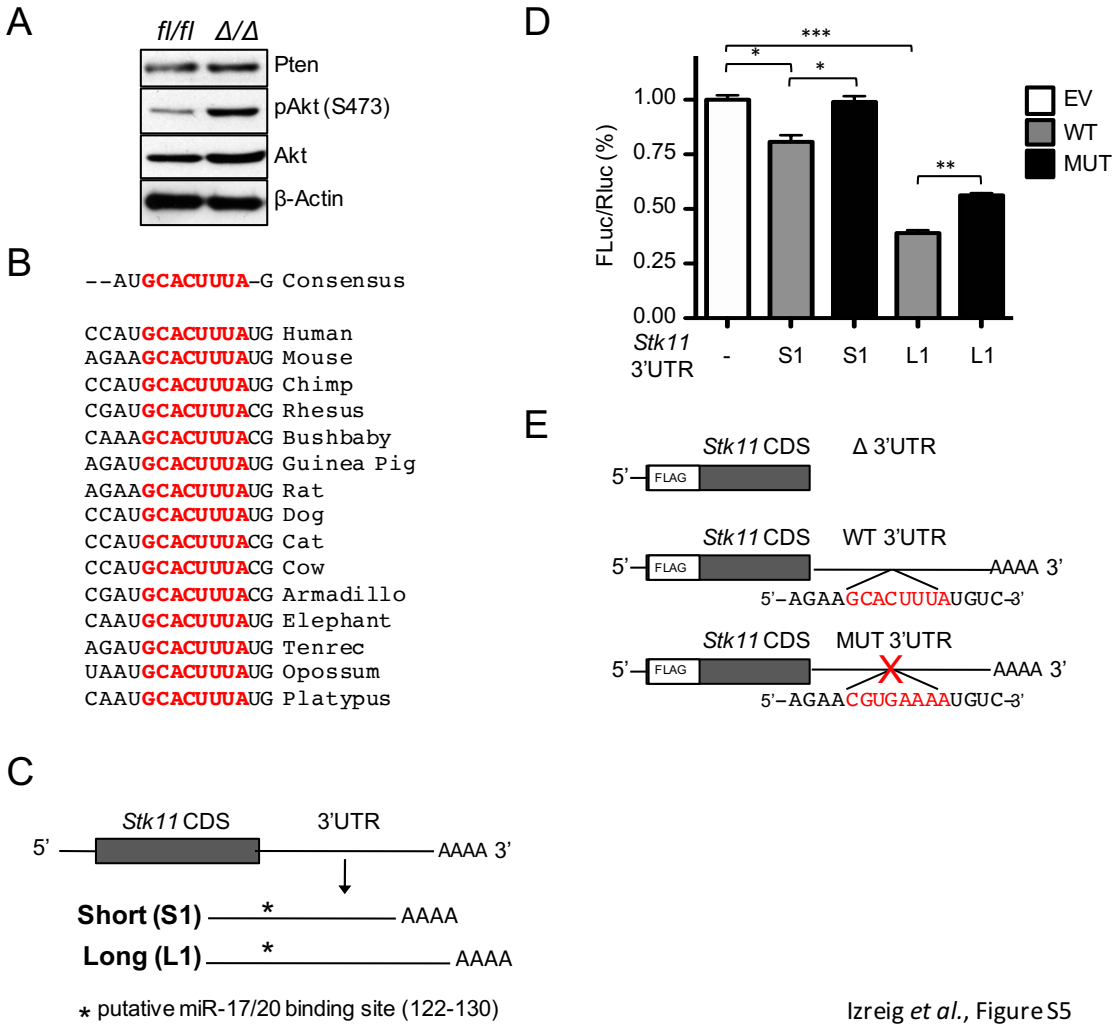

Izreig *et al.*, Figure S5

Figure S6, Related to Figure 7. Knockdown of LKB1 expression restores metabolic activity in *Δ/Δ* lymphoma cells.

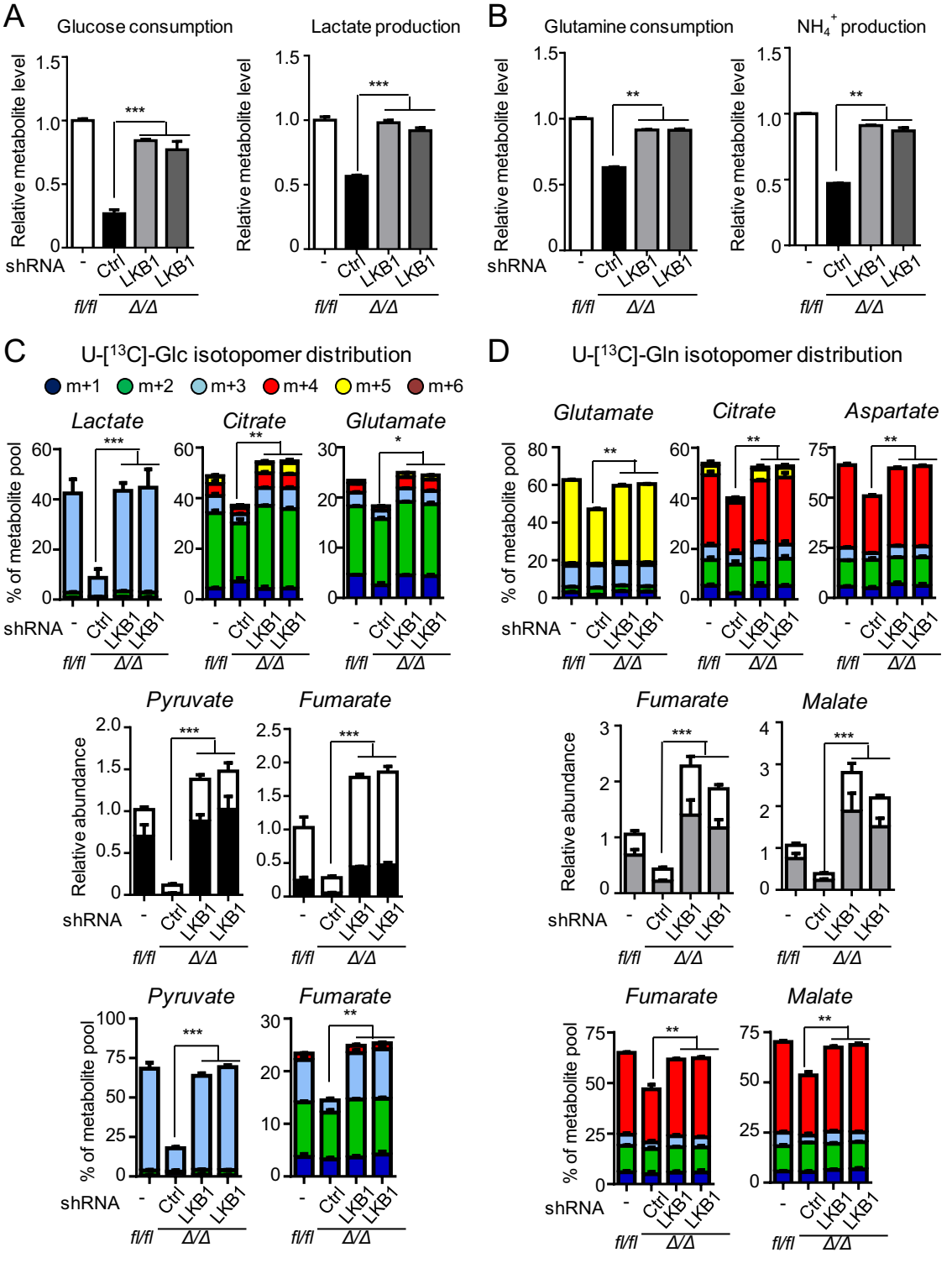

Izreig *et al.*, Figure S6

Supplementary Tables

Table S1. Related to Figure 2. List of differentially regulated genes in Eμ-Myc lymphoma cells expressing (*fl/fl*) or lacking (*Δ/Δ*) *miR-17~92.*

Table S2. Related to Figure 2. List of differentially expressed Myc target genes in Eμ-Myc lymphoma cells expressing (*fl/fl*) or lacking (*Δ/Δ*) *miR-17~92.*

Supplementary Methods

Cell lines, DNA constructs, and cell culture

The generation of Eμ-Myc *Cre-ERT2*$^{+}$;*miR-17~92*$^{fl/fl}$ lymphoma cells has been described previously (Mu et al., 2009). Deletion of *miR-17~92* was achieved by culturing Eμ-Myc *Cre-ERT2*$^{+}$;*miR-17~92*$^{fl/fl}$ cells with 250 nM 4-OHT for four days (Mu et al., 2009), followed by subcloning 4-OHT-treated cells to isolate cells deficient for *miR-17~92*. Eμ-Myc cells were cultured on a layer of irradiated *Ink4a*-null MEF feeder cells in DMEM and IMDM medium (50:50 mix) supplemented with 10% fetal bovine serum (FBS), 20000U/ml penicillin, 7mM streptomycin, 2mM glutamine, and β-mercaptoethanol. Raji cells were cultured in RPMI medium supplemented with 10% FBS, 20000U/ml penicillin, 7mM streptomycin, and 2mM glutamine. Cells were grown at 37°C in a humidified atmosphere supplemented with 5% (v/v) CO_2. For metabolomics experiments using ^{13}C-labelled glucose or glutamine, cells were cultured in glucose- and glutamine-free DMEM/IMDM (50:50 mix) containing 20000U/ml penicillin, 7mM streptomycin, 10% dialysed FBS (Wisent Bio Products), with glutamine (2 mM) or

glucose (25 mM) added back to the medium depending on the tracer used.

Retroviral-mediated gene transfer into lymphoma cells was conducted as previously described (Faubert et al., 2013). Briefly, lymphoma cells were transduced via spin infection, followed by culture in 4 μg/mL puromycin for four days, and subsequent subcloning by limiting dilution. *miR-17~92* deletion constructs have been previously described (Mu et al., 2009). Knockdown of *Stk11* via shRNA (sequence: 5'- AGGTCAAGATCCTCAAGAAGAA -3') was achieved using the miR-30-adapted LMP retroviral vector system (Dickins et al., 2005).

Cell proliferation, cell size, and viability assays

Cells were seeded at a density of 1 x 10^5 cells/mL in 3.5 cm dishes, and cell counts determined via trypan blue exclusion using a TC20 Automated Cell Counter (Biorad). For viability measurements, cells were stained with Fixable Viability Dye eFluor 780 (eBioscience), and analyzed using a Gallios flow cytometer (Beckman Coulter, Fullerton, CA) and FlowJo software (Tree Star, Ashland, OR). Cell size was determined by forward scatter using flow cytometry.

Seahorse analysis and metabolic assays

Cellular oxygen consumption rate (OCR) and extracellular acidification rate (ECAR) were determined using an XF96 Extracellular Flux Analyzer (Seahorse Bioscience) using established protocols (Faubert et al., 2014; Vincent et al., 2015). In brief, 7.5 x 10^4 lymphoma cells were plated per well of an XF96 Seahorse plate in 140 μL of unbuffered DMEM containing 25 mM glucose and 2 mM glutamine, followed by centrifugation at 500xg for five minutes. Seahorse plates were pre-coated with poly-D-lysine (Sigma-Aldrich) to enhance cell adherence. XF assays

consisted of sequential mix (3 min), pause (3 min), and measurement (5 min) cycles, allowing for determination of OCR and ECAR every 10 min. For media metabolite determination, cells were seeded at 1 x 10^5 cells/mL in 3.5 cm plates, and cultured for two days prior to harvesting medium. Culture medium was analyzed for extracellular metabolites (glucose, glutamine, lactate, and ammonia) using a BioProfile Analyzer (NOVA Biomedical) and normalized to cell number, as previously described (Vincent et al., 2015).

GC-MS analysis of ^{13}C-labelled metabolites

Cellular metabolites were extracted and analyzed by GC-MS using previously described protocols (Dupuy et al., 2013; Faubert et al., 2014; McGuirk et al., 2013). For SITA experiments, cells (3-5 × 10^6 per 3.5 cm dish) were incubated for to 2 hours in medium containing 10% dialyzed FBS and either uniformly labeled [^{13}C]-glucose or [^{13}C]-glutamine (Cambridge Isotope Laboratories). Cells were washed twice with saline, then lysed in ice-cold 80% methanol and sonicated. For GC-MS analysis, D-myristic acid (750 ng/sample) was added to metabolite extracts as an internal standard prior to drying samples under a N_2 stream. Dried extracts were dissolved in 30 μL methoxyamine hydrochloride (10 mg/ml) in pyridine and derivatized as tert-butyldimethylsilyl (TBDMS) esters using 70 μL N-(*tert*-butyldimethylsilyl)-N-methyltrifluoroacetamide (MTBSTFA). An Agilent 5975C GC-MS equipped with a DB-5MS+DG (30 m x 250 μm x 0.25 μm) capillary column (Agilent J&W, Santa Clara, CA, USA) was used for all GC-MS experiments, and data collected by electron impact set at 70 eV. A total of 1 μL of derivatized sample was injected per run in splitless mode with inlet temperature set to 280˚C, using helium as a carrier gas with a flow rate of 1.5512 mL/min (rate at which myristic

acid elutes at 17.94 min). The quadrupole was set at 150˚C and the GC/MS interface at 285˚C. The oven program for all metabolite analyses started at 60˚C held for 1 min, then increasing at a rate of 10˚C/min until 320˚C. Bake-out was at 320˚C for 10 min. Sample data were acquired in scan mode (1-600 m/z) (McGuirk et al., 2013). Mass isotopomer distribution for TCA cycle intermediates was determined using a custom algorithm developed at McGill University (McGuirk et al., 2013). After correction for natural ^{13}C abundances, a comparison was made between non-labeled (^{12}C) and ^{13}C-labeled abundances for each metabolite. Metabolite abundance was expressed relative to the internal standard (D-myristic acid) and normalized to cell number.

RNA-Seq analysis and metabolic network integration

RNA preparation and library construction was conducted as previously described (Jha et al., 2015). Briefly, lymphoma cells were seeded at 1 x 10^5 cells/mL, and RNA isolated from cells after two days of culture. For cDNA synthesis, custom oligo-dT primers with barcode and adapter-linker sequences (CCTACACGACGCTCTTCCGATCT—XXXXXXXX-T15) were used. After first strand synthesis, samples were pooled together based on *Actb* qPCR values, and RNA-DNA hybrids degraded using consecutive acid-alkali treatment. A second sequencing linker (AGATCGGAAGAGCACACGTCTG) was ligated using T4 ligase (NEB) followed by SPRI clean-up. The mixture was then PCR enriched for 12 cycles and SPRI purified to yield final strand specific RNA-seq libraries as previously described (Jha et al., 2015). Libraries were sequenced using a HiSeq 2500 (Illumina) using 50bpX25bp pair-end sequencing. Second mate was used for sample demultiplexing, at which point individual single-end fastqs were aligned to mm9 genome using TopHat. Gene expression was obtained using ht-seq and DESeq2 for

differential expression. GSEA on RNA-seq data was conducted using the gage function and non-parametric Kolmogorov-Smirnov test from the GAGE R Bioconductor package (Luo et al., 2009). Network integration of RNA-seq and metabolite datasets was conducted as previously described (Jha et al., 2015).

Immunoblotting and Quantitative Real-Time PCR

Lymphoma cell lines were subjected to SDS-PAGE and immunoblotting using CHAPS and AMPK lysis buffers as previously described (Faubert et al., 2013). Primary antibodies against hexokinase 2, aldolase, LDHA, GLS2, β-actin, 4EBP (total, phospho-T36/47, and phospho-S65), rS6 (total and p S235/236), ULK (total and pS555), Raptor (total and pS792), AMPKα (total and phospho-T172), and FLAG-tag were obtained from Cell Signaling Technology (Danvers, MA). Primary antibody against LKB1 (Ley 37D/G6) was obtained from Santa Cruz Biotechnology (Dallas, TX, USA). For qPCR quantification of mature miRNAs, Qiazol was used isolate RNA, miRNEasy Mini kit was used to purify miRNAs and total mRNA, and cDNA synthesized using the miScript II RT kit (Qiagen). Quantitative PCR was performed using the SensiFAST SYBR Hi-ROX kit (Bioline) and an AriaMX Real Time Pcr system (Agilent Technologies). miScript primer assays (Qiagen) were used to detect mature miRNAs of the *miR-17~92* cluster, with miRNA expression normalized relative to U6 RNA levels.

3'UTR cloning and validation

3'UTR isoforms for mouse *Stk11* were determined by 3'RACE as previously described (Wu et al., 2010). GeneArt DNA fragments (Life Technologies) for either the wild-type *Stk11* 3'UTR or harboring a mutated *miR-17* seed region (bases 2-8 in the seed region) were cloned into the

XhoI/XbaI sites of the pmirGLO vector (Promega). 293T cells (10^5 cells/well) stably expressing FLAG-Ago2 (Valdmanis et al., 2012) were transfected with individual pmirGLO-3'UTR constructs with or without co-transfection of a *miR-17* expression plasmid (*miR-17x4*) (Hong et al., 2010). Cells were lysed 48 hours post-transfection, and the ratio of luciferase to renilla luciferase activity determined using a Dual-Glo Luciferase assay kit (Promega) and a FLUOstar Omega plate reader. FLAG-tagged LKB1 expression constructs were generated by PCR amplification of the full-length LKB1 coding sequence from Eμ-Myc lymphoma RNA, using sequence specific primers to amplify inserts with short or long forms of the *Stk11* 3'UTR.

Tumor xenograft assays

Lymphoma cells were resuspended in HBSS at a concentration of 5 x 10^6 cells/mL, and 10^6 cells/200μl were injected intravenously into CD-1 nude mice (Charles River). Tumor onset was monitored by palpation of inguinal and axillary lymph nodes, and tumor-free survival scored as the time elapsed between injection and first detection of palpable tumors as previously described (Faubert et al., 2013). All procedures were carried out in accordance with guidelines of the Canadian Council on Animal Care, as approved by the Animal Care Committee of McGill University.

Statistical Analysis

Statistics were determined using paired Student's t-test, ANOVA, or Log-rank (Mantel–Cox) using Prism software (GraphPad) unless otherwise stated. Data are calculated as the mean ± SEM for biological triplicates, and the mean ± SD for technical replicates unless otherwise stated. Statistical significance is represented in figures by: *, $p<0.05$; **, $p<0.01$; ***, $p<0.001$;

****, $p<0.0001$.

List of qPCR primers

Gene	Forward Primer	Reverse Primer
Stk11	TTGGGCCTTTTCTCCGAGG	CAGGTCCCCCATCAGGTACT
β-Actin	ATGCTCCCCGGGCTGTAT	CATAGGAGTCCTTCTGACCCATTC

References

Dickins, R.A., Hemann, M.T., Zilfou, J.T., Simpson, D.R., Ibarra, I., Hannon, G.J., and Lowe, S.W. (2005). Probing tumor phenotypes using stable and regulated synthetic microRNA precursors. Nature genetics *37*, 1289-1295.

Dupuy, F., Griss, T., Blagih, J., Bridon, G., Avizonis, D., Ling, C., Dong, Z., Siwak, D.R., Annis, M.G., Mills, G.B.*, et al.* (2013). LKB1 is a central regulator of tumor initiation and pro-growth metabolism in ErbB2-mediated breast cancer. Cancer & metabolism *1*, 18.

Faubert, B., Boily, G., Izreig, S., Griss, T., Samborska, B., Dong, Z., Dupuy, F., Chambers, C., Fuerth, B.J., Viollet, B.*, et al.* (2013). AMPK Is a Negative Regulator of the Warburg Effect and Suppresses Tumor Growth In Vivo. Cell Metab *17*, 113-124.

Faubert, B., Vincent, E.E., Griss, T., Samborska, B., Izreig, S., Svensson, R.U., Mamer, O.A., Avizonis, D., Shackelford, D.B., Shaw, R.J.*, et al.* (2014). Loss of the tumor suppressor LKB1 promotes metabolic reprogramming of cancer cells via HIF-1alpha. Proc Natl Acad Sci U S A *111*, 2554-2559.

Hong, L., Lai, M., Chen, M., Xie, C., Liao, R., Kang, Y.J., Xiao, C., Hu, W.Y., Han, J., and Sun, P. (2010). The miR-17-92 cluster of microRNAs confers tumorigenicity by inhibiting oncogene-induced senescence. Cancer Res *70*, 8547-8557.

Jha, A.K., Huang, S.C., Sergushichev, A., Lampropoulou, V., Ivanova, Y., Loginicheva, E., Chmielewski, K., Stewart, K.M., Ashall, J., Everts, B.*, et al.* (2015). Network integration of parallel metabolic and transcriptional data reveals metabolic modules that regulate macrophage polarization. Immunity *42*, 419-430.

Luo, W., Friedman, M.S., Shedden, K., Hankenson, K.D., and Woolf, P.J. (2009). GAGE: generally applicable gene set enrichment for pathway analysis. BMC bioinformatics *10*, 161.

McGuirk, S., Gravel, S.P., Deblois, G., Papadopoli, D.J., Faubert, B., Wegner, A., Hiller, K., Avizonis, D., Akavia, U.D., Jones, R.G.*, et al.* (2013). PGC-1alpha supports glutamine metabolism in breast cancer. Cancer & metabolism *1*, 22.

Mu, P., Han, Y.C., Betel, D., Yao, E., Squatrito, M., Ogrodowski, P., de Stanchina, E., D'Andrea, A., Sander, C., and Ventura, A. (2009). Genetic dissection of the miR-17~92 cluster of microRNAs in Myc-induced B-cell lymphomas. Genes Dev *23*, 2806-2811.

Valdmanis, P.N., Gu, S., Schuermann, N., Sethupathy, P., Grimm, D., and Kay, M.A. (2012). Expression determinants of mammalian argonaute proteins in mediating gene silencing. Nucleic acids research *40*, 3704-3713.

Vincent, E.E., Coelho, P.P., Blagih, J., Griss, T., Viollet, B., and Jones, R.G. (2015). Differential effects of AMPK agonists on cell growth and metabolism. Oncogene *34*, 3627-3639.

Wu, E., Thivierge, C., Flamand, M., Mathonnet, G., Vashisht, A.A., Wohlschlegel, J., Fabian, M.R., Sonenberg, N., and Duchaine, T.F. (2010). Pervasive and cooperative deadenylation of 3'UTRs by embryonic microRNA families. Mol Cell *40*, 558-570.